European Journal of Taxonomy 823: 82–101
https://doi.org/10.5852/ejt.2022.823.1817
ISSN 2118-9773
www.europeanjournaloftaxonomy.eu
2022 · Troya A. *et al.*

Research article

urn:lsid:zoobank.org:pub:FBC9EB23-E4A3-4A06-9EF8-A2908159B3F2

Igaponera curiosa, a new ponerine genus (Hymenoptera: Formicidae) from the Amazon

Adrian TROYA [1,*], Frederico MARCINEIRO [2], John E. LATTKE [3,*] & John LONGINO [4]

[1,2,3] Departamento de Zoologia, Universidade Federal de Paraná, CP 19020, Curitiba, PR, 81531-980, Brazil.
[1] Departamento de Biología, Escuela Politécnica Nacional, Quito, Ecuador, Ladrón de Guevara, E11-253, P.O. Box 17-01-2759, Quito, Ecuador.
[4] Department of Biology, University of Utah, Salt Lake City, Utah, 84112, USA.

[*] Corresponding authors: adrian.troya77@gmail.com; piquihuye@gmail.com
[2] Email: frederico.marcineiro@gmail.com
[4] Email: jacklongino@gmail.com

[1] urn:lsid:zoobank.org:author:5D3CB9AB-818B-4F70-908B-B6F5EF58720E
[2] urn:lsid:zoobank.org:author:6F5BA200-E5FA-4673-8A73-326F71572504
[3] urn:lsid:zoobank.org:author:F5D4A4F1-1C5A-4807-986B-99FE3D1C3DED
[4] urn:lsid:zoobank.org:author:AB5CAEC7-3E62-415C-8ADA-92ED739BB0A2

Abstract. The monotypic ant genus *Igaponera* gen. nov. is proposed to include its type species *I. curiosa* (Mackay & Mackay, 2010). *Igaponera* gen. nov. is described and phylogenetically compared with other ponerine genera based on external morphology. The type species is known from a single gyne originally described in the genus *Pachycondyla* Smith, 1858. *Igaponera curiosa* is easily diagnosed by: costate sculpture on head, mesosoma, and petiole; short, robust, triangular mandibles with blunt apex; relatively large eyes set at mid-length on sides of head; lack of stridulitrum; and presence of distinct but relatively small arolia. Putative apomorphies of the new genus are: cuticular flange concealing metapleural gland opening; vertically standing hypostomal tooth with recessed base; stout mandibular shape with blunt apex; absence of stout spine-like setae on meso- and metatibial apices. Our phylogenetic results based on morphology suggest that *Neoponera* Emery, 1901 and *Pachycondyla* are the closest lineages to *Igaponera,* which shows intermediate characteristics as compared to those genera. The genus is apparently arboreal, known only from a seasonally flooded Igapó forest near Manaus, Brazil. Despite the collection site being frequented by researchers, no other specimens of this genus have been collected in over 40 years prior to this study.

Key words. Amazonas, ant, identification, Neotropics, taxonomy.

Troya A., Marcineiro F., Lattke J.E. & Longino J. 2022. *Igaponera curiosa*, a new ponerine genus (Hymenoptera: Formicidae) from the Amazon. *European Journal of Taxonomy* 823: 82–101.
https://doi.org/10.5852/ejt.2022.823.1817

Introduction

Schmidt & Shattuck (2014) revised the genera of the subfamily Ponerinae, and one of the many important outcomes of their work was the division of the genus *Pachycondyla* Smith, 1858 into 19 putatively monophyletic genera, reflecting the results of molecular studies by Schmidt (2013). This was a long overdue change, as the paraphyly of *Pachycondyla* had been either implied or explicitly recognized in previous studies (Wild 2005; MacKay & MacKay 2010; Keller 2011; Mariano *et al.* 2011). Their significant results notwithstanding, the authors pointed out that additional work was still necessary due to problems such as insufficient sampling. Schmidt & Shattuck (2014) reduced *Pachycondyla* from 90 to 17 extant species and placed the genus within the "*Pachycondyla* genus group", one of six informal groups within the subtribe Ponerini, which was recently reaffirmed in Branstetter & Longino (2022). The *Pachycondyla* genus group comprises seven genera: *Belonopelta* Mayr, 1870, *Dinoponera* Roger, 1861, *Mayaponera* Schmidt & Shattuck, 2014, *Neoponera* Emery, 1901, *Pachycondyla*, *Simopelta* Mann, 1922, and *Thaumatomyrmex* Mayr, 1887. Their (i.e., Schmidt & Shattuck 2014) definition of the genus *Pachycondyla* largely coincided with that of the *crassinoda* species complex as defined by Mackay & Mackay (2010) in the latest revision of *Pachycondyla*. However, one species that Schmidt & Shattuck (2014) left in *Pachycondyla* was *P. curiosa*, which was described by Mackay & Mackay (2010) and placed in its own species complex, because they could not find any affinity with the other species they studied. Schmidt & Shattuck (2014) also had their doubts about the position of this species within the genus, but it was provisionally left in *Pachycondyla*, since they could not examine the specimen at the time. Recently, Esteves & Fisher (2021) placed *P. curiosa* in the genus *Neoponera*, although without a thorough examination of the specimen voucher (LACM-ENT226103). The original species description is based on a single specimen collected in a seasonally flooded forest near Manaus, Brazil, a dealate female deposited in the Entomological Collection of the Los Angeles County Museum of Natural History, California, U.S.A. The external morphology of the specimen was studied with the objective of determining its affinities with other ponerines. We conclude that it represents an unknown genus lineage of the tribe Ponerini. It is transferred out of *Neoponera* into its own genus, which is diagnosed and compared with other genera that could either be closely related to it or possibly confused with it.

Material and methods

The point mounted specimen (holotype of *Igaponera curiosa*) was sent to the Longino Lab, University of Utah, U.S.A., remounted and then studied using a Leica M80 binocular stereoscope with a 10x ocular lens and an x-y sliding stage fitted with a Mitutoyo micrometer for each axis. The images in Fig. 3 (A–D) are composites created using Leica Application Suite V3.7 from source images taken with a Leica Z16 APO stereo microscope adapted with a Leica DCF450 camera. Additional images of this ant are available on AntWeb.org (www.antweb.org, LACM-ENT226103). Morphological terms mostly follow Delsinne *et al.* (2019) for general morphology, Richter *et al.* (2019) for head morphology, and Harris (1979) for sculpturing.

The specimen was subjected to non-destructive DNA extraction using a Qiagen DNA extraction kit, but no DNA was detected. Thus, our phylogenetic analyses (see below) are based entirely on morphology.

We studied the morphology of 136 specimens (43 gynes and 93 workers) representing 91 ponerine species (Table 1; Supp. file 3). These specimens are all permanently or temporarily deposited in the DZUP entomological collection, Universidade Federal do Paraná, Curitiba, Brazil, or in the Longino Lab, University of Utah, USA.

Phylogenetic analyses

In order to infer the approximate phylogenetic placement of *Igaponera* gen. nov. within the Ponerinae, we made a morphological analysis mostly based on the data set of Keller (2011) and other authors, but

Table 1. Ponerine taxa examined. In bold: included in the phylogenetic analysis; *: only worker caste available; [1], examined through SEM images from AntWeb; E&F: Esteves & Fisher; M&M: Mackay & Mackay.

Bothroponera soror* Emery	*Neoponera emiliae* Forel*	***Neoponera venusta* Forel***
Brachyponera chinensis* (Emery)	*Neoponera fauveli* (Emery)*	***Neoponera villosa* (Fabricius)**
Centromyrmex gigas* Forel	*Neoponera fisheri* M&M	***Odontomachus bauri* Emery***
***Corrieopone nouragues* (E&F)**	*Neoponera foetida* (Linnaeus)	*Odontomachus hastatus* Fabricius*
Diacamma ceylonense* Emery	*Neoponera fusca* M&M*	***Odontoponera transversa* (Smith)***
Dinoponera grandis* Guérin-Méneville	*Neoponera globularia* M&M	***Pachycondyla crassinoda* (Latreille)**
Dinoponera lucida Emery*	*Neoponera goeldii* Forel	*Pachycondyla harpax* (Fabricius)
Hagensia peringueyi* (Emery)	*Neoponera hispida* M&M*	*Pachycondyla impressa* (Roger)
Harpegnathos saltator* Jerdon	*Neoponera holcotyle* M&M	*Pachycondyla lenkoi* Kempf*
***Hypoponera* sp.**	*Neoponera insignis* M&M	*Pachycondyla procidua* (Emery)
Leptogenys luederwaldti* Forel	*Neoponera inversa* (Smith)	*Pachycondyla striata* Smith
Mayaponera arhuaca (Forel)*	***Neoponera laevigata* (Smith)**	***Paltothyreus tarsatus* (Fabricius)***
***Mayaponera constricta* (Mayr)**	*Neoponera latinoda* M&M	***Phrynoponera gabonensis* (André)***
Megaponera analis (Latreille)*	*Neoponera lineaticeps* (Mayr)*	*Platythyrea conradti* Emery*
Neoponera aenescens (Mayr)	*Neoponera luteola* (Roger)*	***Platythyrea punctata* (Smith)***
Neoponera antecurvata M&M	***Neoponera magnifica* (Borgmeier)***	***Plectroctena subterranea Arnold****
***Neoponera apicalis* (Latreille)**	*Neoponera marginata* (Roger)	***Ponera coarctata* (Latreille)***
Neoponera bactronica Fernandes *et al.*	*Neoponera metanotalis* (Luederwaldt)*	***Psalidomyrmex procerus* Emery***
Neoponera bugabensis (Forel)	*Neoponera moesta* (Mayr)	***Pseudoneoponera tridentata* (Smith)***
Neoponera carbonaria (Smith)	*Neoponera oberthueri* (Emery)	***Pseudoponera stigma* (Fabricius)***
Neoponera carinulata (Roger)	*Neoponera obscuricornis* (Emery)	*Rasopone ferruginea* (Smith)
Neoponera cavinodis Mann	*Neoponera recava* M&M	***Rasopone lunaris* (Emery)**
Neoponera chyzeri (Forel)	*Neoponera rostrata* (Emery)	*Simopelta oculata Gotwald &* Brown*,[1]
***Neoponera commutata* (Roger)**	*Neoponera rugosula* Emery	***Simopelta pergandei* (Forel)***
Neoponera concava M&M	*Neoponera schoedli* M&M*	***Streblognathus aethiopicus* (Smith)***
Neoponera cooki M&M*	*Neoponera schultzi* M&M*	***Thaumatomyrmex contumax* Kempf***
Neoponera crenata (Roger)	*Neoponera solisi* M&M	*Thaumatomyrmex mutilatus* Mayr*
Neoponera curvinodis (Forel)	*Neoponera striatinodis* (Emery)	*Thaumatomyrmex zeteki* Smith*
Neoponera dismarginata M&M*	*Neoponera theresiae* (Forel)*	***Wadeura holmgreni* (Wheeler)***
Neoponera donosoi M&M*	*Neoponera verenae* Forel	
***Neoponera eleonorae* (Forel)**	***Neoponera unidentata* (Mayr)**	

also on newly coded characters (Supp. file 1 and Supp. file 2). We followed, in general, the guidelines on character coding by Sereno (2007). The 36 ingroup taxa (Table 1; Supp. file 3) represent a wide breadth of ponerine diversity, including lineages from all the informal clades elucidated in Schmidt & Shattuck (2014: Figs. 1–2), plus the recently erected Amazonian genus *Corrieopone* Esteves & Fisher, 2021. With the aim of representing the morphological diversity in *Neoponera*, we also incorporated representatives from nearly all the currently recognized species-groups *sensu* Mackay & Mackay (2010). We did not include the *N. rostrata* group, which contains only two morphologically similar taxa, and is closely related to the *N. crenata* group, which is included in the phylogeny (e.g., *N. unidentata* Mayr, 1862). *Neoponera bucki* Borgmeier, 1927, assigned to the "*Pachycondyla stigma* species-complex" *sensu* Mackay & Mackay (2010), was also not considered here since its morphology departs from the actual taxonomic limits of *Neoponera*, and it is distantly related to it (pers. obs.).

Using the visual character diagnoser implemented in WINCLADA ver. 1.00.08 (Nixon 2002), we first discarded the parsimony-uninformative characters, including those that are autapomorphic, from an initial character set. Our final matrix was then composed of 36 characters showing topological correspondence among all the terminals in our data set including two outgroups, *Paraponera clavata* (Fabricius, 1775) and *Tatuidris tatusia* Brown & Kempf, 1968, which we chose based on the hypotheses of Keller (2011) and Branstetter *et al.* (2017). Most character statements represent fairly discernible external body structures, which can be replicated in future studies.

The matrix was constructed in Excel, edited in Mesquite ver. 3.6 (Maddison & Maddison 2019), and analyzed using two methods of phylogenetic inference: maximum likelihood (ML) in IQ-TREE 2.1.2 (Nguyen *et al.* 2015) through the CIPRES Science Gateway ver. 3.3 (phylo.org), and maximum parsimony (MP) in TNT ver. 1.5 (Goloboff & Catalano 2016). We applied the following ML parameters in our analysis: morphological (also known as "standard") sequence type; branch support calculated with 1000 ultrafast bootstrap (UFB) (Hoang *et al.* 2018) replicates (also referred to as "samples") in 1000 iterations with a minimum correlation coefficient of 0.99; we limited the tree search to 100 unsuccessful iterations with a perturbation strength of 0.3 to 0.5; to infer single-branch supports we chose the SH-approximate likelihood ratio test (SH-aLRT) (Guindon *et al.* 2010), approximate Bayes test (aBayes) (Anisimova *et al.* 2011), and fast local bootstrap test (FB); Model Finder (Kalyaanamoorthy *et al.* 2017) tested 22 morphological models (by default) under the Akaike information criterion (AIC) (Akaike 1973) and the Bayesian information criterion (BIC) (Schwarz 1978).

MP analyses were conducted using the "traditional" heuristic tree search method both under equal and implied weights. In a series of runs, we set the value of the concavity function *k* between 1–20 and 50, all returning incongruent or non-resolved topologies. We then used the script setk.run (anonymous author) (Supp. file 5), which returned an appropriate, more precise value of *k*, thus optimizing the resulting most parsimonious tree topologies. An alternative to said script is using the extended implied weighting (xpiwe) TNT function (Goloboff 2014). With the former option, however, we obtained more congruent and resolved trees. Tree searches consisted of 100 to 10 000 rounds of random addition sequences, followed by tree bisection reconnection (TBR) branch swapping, saving 10 trees per replication. Remaining tree search parameters were left as the default values. In addition, we conducted tree searches using the "new technology" method with both equal and implied character weighting. The resulting trees, though, were less resolved as compared to those obtained with the traditional search method. Branch supports were estimated with bootstrap (Felsenstein 1985) and symmetric resampling (Goloboff *et al.* 2003). We used WINCLADA to visualize ancestral states across the final tree topology, as well as to illustrate non-homoplastic apomorphies and homoplasies. The final cladograms were edited with FigTree ver. 1.4.4 (http://tree.bio.ed.ac.uk/software/figtree) and refined using Adobe Illustrator ver. 24.2.3®.

Measurements and indices

CI = Cephalic Index – HW/HL x 100
EL = Eye Length – Maximum length of the eye with head in lateral view
EW = Eye Width – Maximum width of the eye, perpendicular to EL, with head in lateral view
HL = Head Length – Maximum length of the head in dorsal view, excluding the mandibles, from the anteromedian clypeal margin to the mid-point of the posterior margin of the head
HW = Head Width – Maximum width of the head in dorsal view, excluding the eyes. Taken in the same plane as HL
MetL = Metatibial length – Maximum straightline distance from the base of the metatibia to its apex, excluding setae and spurs
MI = Mandibular Index – ML/HL x 100
ML = Mandible length – Distance from the mandibular outer base to the apex of the apical tooth. Taken in the same plane as HL
OI = Ocular Index – EL/HW x 100
PI = Petiolar Index – PW/PL x 100
PH = Petiole Height – Maximum vertical length, with node in lateral view, from the ventral point of the subpetiolar process, excluding the anterior tooth, to the highest point of the node
PL = Petiole Length – Maximum length of the petiole in lateral view from the anterior margin to the posterior margin, excluding the helcium
PrW = Pronotal width – Maximum width of the pronotum in dorsal view
PW = Petiole Width – Maximum width of the petiole in dorsal view

SI = Scape Index – SL/HW x 100
SL = Scape Length – Maximum length of the scape from the base to the apex, excluding the basal constriction
WL = Weber's Length – Length of the mesosoma in lateral view from the anterior margin of the pronotum, excluding the collar, to the posterior margin of the metapleural lobe

Institutions

INPA = Instituto Nacional de Pesquisas da Amazônia

Results

Phylogeny

Summary statistics

ML analysis returned 34 distinct patterns, 35 parsimony-informative sites, and one singleton site. The best-fit model selected by Model Finder was MK+FQ+ASC+G4 according to BIC. After processing 1000 UFB samples, the program made a final optimization of the model parameters and estimated the best log-likelihood (-715.566), which is slightly smaller than that actually found (-715.758) for the consensus tree with length = 4.344. As for MP, the final run under "traditional search" and weighted characters (k = 5.7813) returned 84 equally most parsimonious trees, 8.94 steps in length, with consistency index (CI) = 36, and a retention index (RI) = 59. Specific values of CI and RI for each character in the matrix varied from 9 to 100 ($\bar{x}$ = 49), and from 0 to 100 ($\bar{x}$ = 60), respectively. Characters with very low RI (i.e., = 0), namely, char. 13 and char. 14 (Supp. file 1), were kept in the analysis since these contributed to distinguish between *Igaponera* and its closely related lineages, and between the outgroup *Tatuidris tatusia* and most ingroup lineages, respectively.

Within *Neoponera* the following triads of taxa showed no variation among the set of characters: *Neoponera apicalis* (Latreille, 1802) – *N. commutata* (Roger, 1860) – *N. villosa* (Fabricius, 1804), and *N. eleonorae* (Forel, 1921) – *N. laevigata* (Smith, 1858) – *N. magnifica* (Borgmeier, 1929). The program kept them in the analysis, however, since they differ in character 7 (malar carina: present in the first triad; absent in the second).

Placement of *Igaponera* gen. nov. in Ponerinae and apomorphic traits

The resulting phylogenetic relationships among the examined ponerine lineages were similar in consensus ML and MP trees (Fig. 1). Although the *Pachycondyla* genus group was not recovered as a clade, most of the genera included in it emerged as closely related on our tree topologies, with *Igaponera* placed as an independent lineage relative to its neighboring lineages, *Neoponera* and *Pachycondyla*. The main difference between the two topologies is the placement of the clade *Simopelta* + *Thaumatomyrmex*, which emerged as sister to *Platythyrea*, near the base of our MP tree, whereas on the ML tree those genera are the most derived ones among our examined set. Under the likelihood approach the node linking *Neoponera* and *Igaponera* showed slightly higher support (SH-aLRT: 84, FB: 76, aBayes: 96) than the node linking *Igaponera* and *Pachycondyla* (SH-aLRT: 80, FB: 70, aBayes: 78), with the aBayes test giving good support to the former. Bootstrap and symmetric resampling node supports under parsimony ranged between 70% and 100% in both methods, showing though, unresolved relationships in most ingroup lineages, including those in the *Pachycondyla* genus group Supp. file 4).

Within the *Pachycondyla* group, *Igaponera* shares a number of traits with its closely related lineages, *Neoponera* and *Pachycondyla*; among the most notable that also distinguish them from other ponerines are, for example, the number of maxillary (char. 8) and labial (char. 6) palpomeres (4, 4); a slit-shaped propodeal spiracle (char. 19) whose length is usually three times as long as its width, except for most

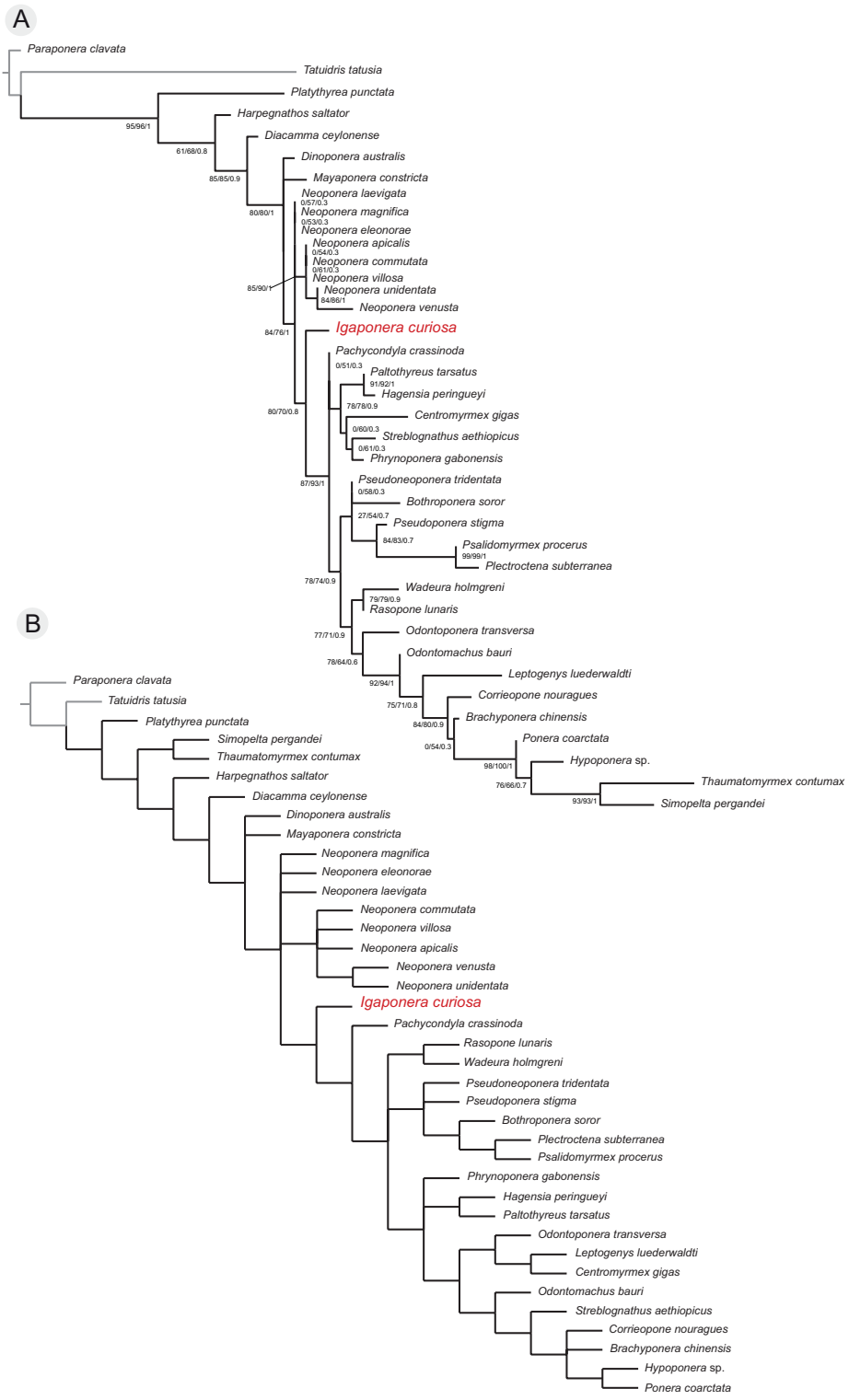

Fig. 1. Morphology-based consensus phylogenies depicting the placement of *Igaponera* gen. nov. within the Ponerinae (Formicidae). The trees were inferred through: **A**. maximum likelihood in IQ-TREE, and **B**. maximum parsimony in TNT, using a data set composed of 36 characters and 38 terminals: 36 ingroup taxa, and two outgroups (branches in grey). The numbers next to nodes represent statistical support (SH-aLRT/Bootstrap/aBayes) and are only provided in the maximum likelihood tree (see Material and methods).

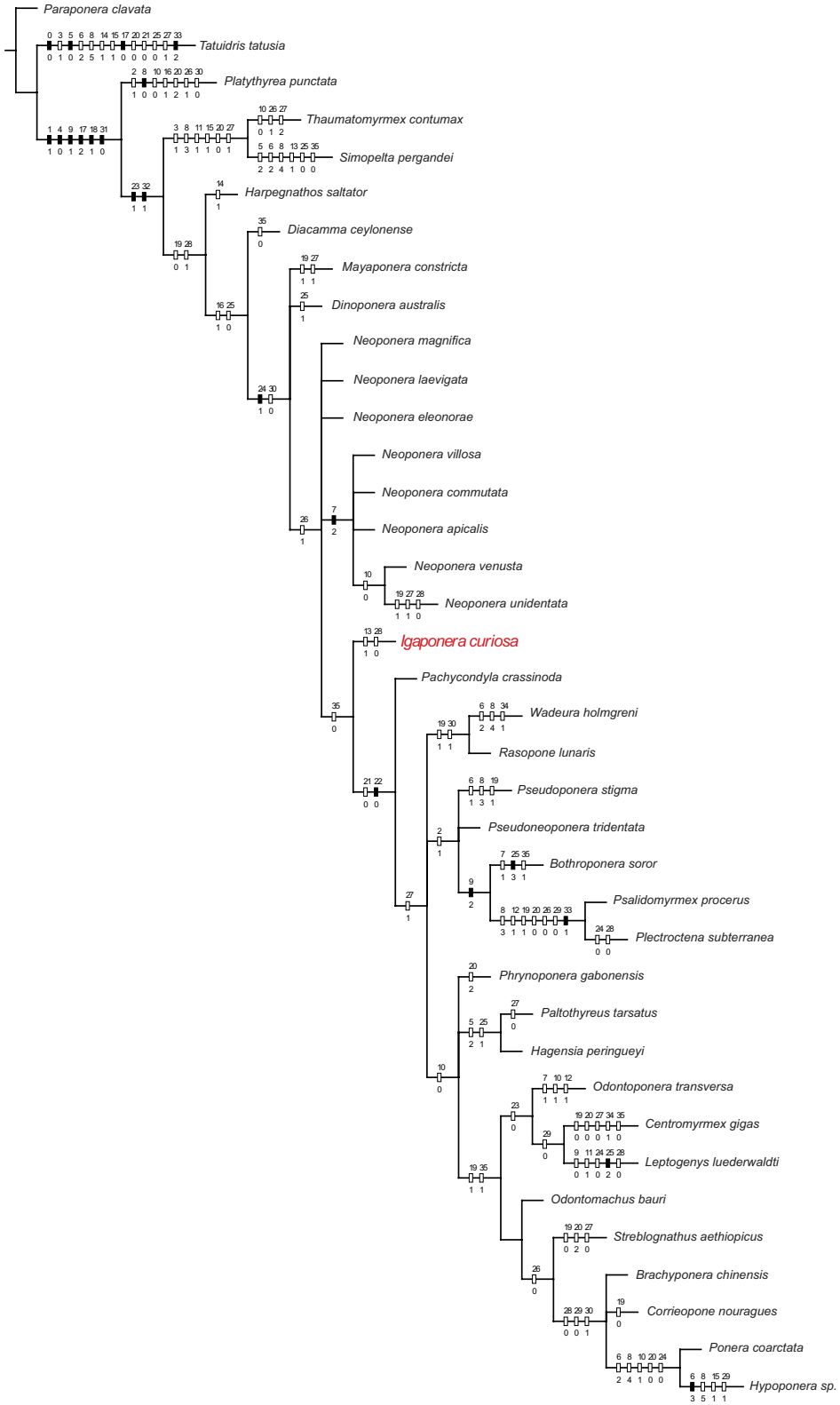

Fig. 2. Strict consensus phylogeny, identical to that in Fig. 1B, obtained through maximum parsimony. The tree shows homoplastic (white square marks) and non-homoplastic (black square marks) apomorphies. Numbers above the marks represent the characters examined, and numbers below the marks represent character states (see also Supp. file 1).

taxa in the *Neoponera emiliae* species group, for example *N. venusta*, *N. metanotalis*, which bear round spiracles; usually a dome-shaped, ventrally striated, and anteriorly carinated subpetiolar process (sternite of abdominal segment II).

Among the shared/not shared traits between *Igaponera* and its closely related lineages, we found, for example, the stridulitrum on the pretergite of abdominal segment IV (char. 35), which is absent in *Igaponera* as well as in all *Pachycondyla* species, but is present in all known *Neoponera*; the pretarsal arolia (chars 21, 22), which are present, though very small, in *Igaponera*, but absent or vestigial in *Pachycondyla*.

The only putative autapomorphy identified in *Igaponera* is the hypostomal tooth with its tip directed ventrally (recessed), not anteriorly or anterolaterally as in all other examined ponerines.

We found the following combination of apomorphies for *Igaponera*, which are not to be found in any other ponerine lineage (Fig. 2; Supp. file 1): 1) a dorsal cuticular flange partially concealing the metapleural gland opening in dorsal view (char. 13); a similar structure is apparent in *Simopelta oculata* Gotwald & Brown, 1967 and *S. pergandei* (Forel, 1909), and possibly in all known *Simopelta*, a distantly related lineage in the *Pachycondyla* group; 2) elongate, flexuous (not spine-like) setae on the meso- and metatarsi, which are present only in all known *Dinoponera* within the *Pachycondyla* group, and outside of it are present in a number of other ponerines; 3) meso- and metatibial apices devoid of stout, spine-like setae (char. 28), which are relatively common structures in many ponerine lineages, but within the *Pachycondyla* group they are also absent in *Simopelta* and *Thaumatomyrmex*. The comparative morphology of these traits is treated in more detail in the Discussion.

Taxonomy

Class Hexapoda Blainville, 1816
Order Hymenoptera, Linnaeus, 1758
Family Formicidae Latreille, 1809
Subfamily Ponerinae Lepeletier de Saint-Fargeau, 1835

Igaponera gen. nov.
urn:lsid:zoobank.org:act:97BBFF3A-4D59-4CA8-9276-170B61AA24B0

Type species

Igaponera curiosa (MacKay & MacKay, 2010).

Diagnosis

- Eye placed slightly anterad of cephalic mid-length, length occupying close to one-third of lateral cephalic margin
- Scape not reaching posterior cephalic margin when pulled posteriorly
- Funicular segments broader than long
- Malar carina absent
- Mandible triangular, relatively short and robust
- Mandible lacking lateral sulcus
- Mandibular apex in dorsal view blunt
- Teeth along masticatory margin short and of similar size
- Lateral hypostomal process (tooth) with tip directed ventrally, not anteriorly or anterolaterally
- Humeral carina absent
- Propodeal spiracle slit-shaped, almost vertical
- Metapleural gland opening facing laterally, dorsally partially covered by low lobe, posteriorly bound by flange with convex lip

- Petiole sessile with blunt anterolateral projection
- Helcium with narrow transverse rugulose strip between pretergite and constriction at anteroventral face of tergite III
- Prora protrudes anteriorly as brief, anteriorly projecting, bluntly pointed lobe with convex ventral face bordered by lip along lateral margin
- Cinctus strongly marked
- Stridulitrum absent
- Epipygium and hypopygium lacking spine-like setae or stout hairs
- Epipygium convex in cross-section, not posteromedially flattened
- Meso- and metatibial apex each with two spurs, one long and pectinate, one short and simple
- Meso- and metatibial apices lacking spine-like setae
- Tarsal setae (except on probasitarsus) elongate and of flexuous appearance, particularly on penultimate tarsomere
- Claws simple with small arolium
- Head, mesosoma, and petiole with longitudinal, parallel, uniform costulae.

Etymology

The genus name is derived from the Brazilian name for black-water flooded forests in the Amazon region, *Igapó*. The suffix "-*ponera*" is derived from the Greek word "poneros" for "wretched", "wicked", "useless". It is commonly used in generic epithets of the subfamily Ponerinae. It is a non-Latinized neologism and thus invariant.

Igaponera curiosa (MacKay & MacKay, 2010)
Fig. 3A–D

Pachycondyla curiosa MacKay & MacKay 2010: 295, figs 423–424. Holotype queen: Brazil, Amazonas, Rio Tarumã-Mirím, Igapó; 6 Jan. 1976; J. Adis leg.; Jt-1. [Los Angeles County Museum of Natural History, unique specimen identifier LACM-ENT226103] (examined).

Neoponera curiosa Mackay & Mackay 2010; Esteves & Fisher 2021: 103 (combination in *Neoponera*).

Diagnosis

As for genus.

Measurements

HL 1.52; HW 1.38; ML 0.74; EL 0.39; EW 0.29; SL 1.07; PrW 1.13; WL 2.43; PH 0.98; PW 0.84; PL 0.79; MetL 1.20. Indices: CI 91; OI 28; MI 49; SI 78; PI 106.

Description

Queen (holotype)

Head (Fig. 3B–C). Subquadrate in dorsal view, posterior margin straight; lateral margin mostly weakly convex, posterolaterally curving mesad. Eye surface convex, shape in perpendicular view elongate ovoid, three-fourths longer than wide. Anterior clypeal margin in dorsal view shaped as broadly obtuse angle with blunt apex. Cephalic dorsum mostly with diverging costae, some longitudinal costae present between ocelli, vertex longitudinally costate. Three relatively small, one-sixth of eye length, similar-sized ocelli placed on posterior third of head, distance between ocelli approximately 3× diameter of each ocellus. Lateral margin of frontal lobe convex, dorsal surface convex with lateral margin higher than mesial margin, dorsum mostly smooth with scattered punctulae; lobe covers most of scape basal condyle in cephalic dorsal view, neck exposed. Genae longitudinally rugulose. Vertexal carina arched.

Fig. 3. *Igaponera curiosa* (Mackay & Mackay, 2010), holotype queen. **A**. Body in dorsal view. **B**. Body in lateral view. **C**. Head in frontal view. **D**. Petiole in lateral view. Additional images available on AntWeb (www.antweb.org). Scale bars: A–B = 1 mm; C–D = 0.5 mm.

Clypeus with lateral surface projecting dorsoanteriorly as inclined shelf, laterally finely rugulose, close to antennal sclerite smooth with punctulae, median clypeus raised with blunt longitudinal shining convexity, anterior margin with coarse punctae. Supraclypeal area extends posteriorly between frontal carinae, slightly surpassing level of anterior eye margin. Scape mostly smooth with abundant piligerous punctulae, gradually widening apicad, surface with abundant appressed pubescense and scattered decumbent and subdecumbent hairs, none longer than scape width. Scape barely reaches posterior cephalic margin when pulled back. Antennomere II elongate campaniform; antennomeres II–IV slightly broader than long, antennomeres V-XII noticeably broader than long, apical antennomere longest, with blunt tip. Each funicular piece with decumbent hairs, especially towards apical margin. Mandible with convex dorsal surface, mostly smooth with scattered elongate punctae, transverse basal ridge present, laterobasal area rugulose and with rounded depression; masticatory margin with 4 short, similar-sized triangular teeth on apex and 5 stout denticles basad to teeth. Cephalic ventral surface mostly flattened with slightly elevated anteromedian triangular-shaped region on hypostomal region; mostly transversely striate, discal area tending to smooth. Postgenal ridge weakly impressed, appearing as series of small, shallow depressions. Labrum broader than long, dorsum mostly smooth and shining, with basal transverse convexity, anteromedially with angular cleft. Prementum smooth and shining, ventral surface convex; medially with tenuous transverse premental groove. Palp formula: 4,4. Hypostoma widest mesad, forming smooth and shining narrow strip, hypostomal tooth with lateral twist, vertical to cephalic ventral surface and with blunt point. Stipes apically bidentate; external margin broadly convex. Cephalic dorsum with abundant erect to suberect anteriorly arching hairs, hairs on cephalic venter straighter and longer. Anterior clypeal margin with long, golden straight setae, and sparse short setae and hairs.

Mesosoma (Fig. 3A–D). Dorsal margin of pronotum, mesonotum and propodeum weakly convex, almost straight. Propodeum convex with declivitous margin longer than dorsal margin. Most of pronotal lateral margin longitudinally irregularly costate, ventrolateral margin bound by sulcus with several transverse ridges; humeral carina completely absent; anepisternum with costae parallel to anapleural sulcus, sulcus broad and deep; katepisternum with oblique to longitudinal costae; anteroventral mesopleural carina distinct. Mesometapleural suture well-impressed, metapleuron and lateral propodeal face with oblique irregular costae; metapleural-propodeal suture weakly impressed. Pronotal dorsum with concentric anteriorly convex costae. Most of mesonotum longitudinally costate, costae slightly arched along lateral margins of scutum. Transcutal suture fine but distinct, scutoscutellar sulcus broad and shallow, not breaking costae. Metanotum transverse, longitudinally costulate. Wing stumps evident. Propleuron transversely costate, anterior one-third narrow, anterior surface in lateral view bent at approximately 120° angle to posterior surface. Prosternum shaped as ventroposteriorly pointing triangular lobe in ventral view. Ventral surface of mesopleuron transversely costate. Mesocoxa anteriorly bound by mesosternal process shaped as elongate right triangle with blunt apex; metasternal process shaped as bluntly-pointed, flattened lobe; metacoxal cavity closed. Propodeal spiracle slightly protruding, opening directed posterolaterally; spiracle situated at propodeal midlength, close to metapleuron. Propodeal dorsal and declivitous faces transversely costate, separation between lateral and declivitous surfaces bluntly angular; dorsal face shorter than declivitous face. Metapleural ventral margin bordered by broad, shallow sulcus.

Legs (Fig. 3A, B). Protibial apex with single preapical seta and robust, apically pectinate calcar with basal velum; posterior margin of velum slightly rounded and shorter than anterior pointed margin; strigil comb opposite calcar with row of tooth-like setae, posterior basitarsal face, distad of comb, densely clothed with decumbent appressed golden hairs. Procoxa and profemur mostly smooth and shining, protibia densely punctulate. Meso- and metatarsi with abundant hairs, some relatively thick, but none shaped as short, stout, spine-like setae. Length of arolium not more than one fourth of claw length.

Petiole (Fig. 3A–B, D). Sessile; node in lateral view subquadrate, higher posterad than anterad; anterior margin vertical, weakly concave; dorsal margin weakly convex, posterior margin vertical. Node

anterolaterally with short, robust projection, spiracle placed just posterad to projection; lateral nodal face longitudinally costate on ventral half, costae oblique and thicker on dorsal half. Tergosternal suture well-marked. Petiolar sternite projects ventrally as broad longitudinal ridge with transverse costae; ventral margin of sternite in lateral view broadly convex with brief carinate concavity just posterad of anterior process; petiolar process in lateral view with convex anterior margin ending in brief posteriorly curved point; process in ventral view forms anteriorly-pointing angle. Node in dorsal view shaped as robust isosceles trapezoid, slightly wider posterad, anterior petiolar margin concave with incomplete transverse carina, anterior margin of node broadly convex, lateral margin broadly convex, posterior margin straight. Dorsal face mostly transversely costate with posterior costae arched. Anterior and posterior faces transversely costate. Petiole without posterior shelf.

Gaster (Fig. 3B, D). Helcium low on anterior face of abdominal segment III, pretergite overlapping presternite. Anterior margin of abdominal tergite III in lateral view straight, vertical, forming blunt, obtuse angle with dorsal margin; most of sternoventral margin broadly convex. Dorsal gastral margin in lateral view mostly convex, dorsal margin of abdominal segment IV 2× as long as ventral margin. Gaster mostly smooth and shining with scattered shallow, piligerous punctae; dorsum of abdominal tergite III with more abundant and slightly deeper punctae than on tergite IV; anterior face of tergite III flattened, without piligerous punctae. Spiracles visible on abdominal segments III, IV, and V. Epipygium mostly smooth and shining, broadly convex in transverse section, not laterally compressed, posterolaterally with fine striae converging posteriorly towards stinger with smooth patch in middle; short posteromedian longitudinal carina present, less than one-eighth length of epipygium, ventrolaterally with abundant punctae; robust sting, surrounded by abundant short hairs.

Pilosity. Mesosoma, legs, and node with abundant short decumbent pilosity, mesosoma in lateral view with abundant erect and suberect hairs; gaster with sparse appressed pilosity mostly on third tergite, rest with abundant erect to suberect hairs. Anterior and posterior faces of meso- and metacoxa densely pubescent.

Color. Head, mesosoma, and petiole black; mandible ferruginous, masticatory margin dark brown; palps yellow; antenna and legs dark ferruginous brown; gaster ferruginous brown. Masticatory margin darker than rest of dorsal mandibular surface.

Discussion

Phylogeny

In the genomics era, morphology-based phylogenies are increasingly uncommon, particularly when dealing with hundreds or even thousands of taxa (e.g., Pyron *et al.* 2013; Wiemers *et al.* 2020). Testing relationships based on scored character statements is thus generally the norm when organisms with low-quality or degraded DNA are at play. Although the morphological data set we used was small, as compared, for example, to that of Keller (2011) where the author used 139 character statements, it is enough to inform us about the approximate placement of a rare specimen within the Ponerinae.

Although the statistical resampling returned unresolved, but relatively well supported topologies under parsimony, the more resolved, though not strongly supported topology, under the likelihood approach, partially sustains our hypothesis in regards to the independence of *Igaponera* from its closest lineages, *Neoponera* and *Pachycondyla*. With the following arguments, we further support this phylogenetic inference:

The strongly costate sculpture of *Igaponera* is definitely an unusual trait for a *Pachycondyla* group member, or even for a ponerine! However, based on its overall external body features, we found this lineage to be similar in appearance to only three genus lineages within the *Pachycondyla* group:

Mayaponera, *Neoponera*, and *Pachycondyla*. Among them, the latter two display more similarities with the new genus, and the following characters can be considered useful for distinguishing their close relationship.

The lobate projections on the fourth protarsomere (char. 27, state 0) is a trait shared among *Igaponera*, *Neoponera*, *Pachycondyla*, and *Dinoponera*. The trait is conical (state 1) in *Mayaponera*, whereas in *Simopelta* and *Thaumatomyrmex*, here considered distantly related to *Igaponera*, it is cylindrical (state 2). According to Keller (2011), these transformations are additive, and based on the phylogenies of Schmidt & Shattuck (2014) and Branstetter & Longino (2022), the cylindrical condition is ancestral to a more derived lobate structure which is present in what could be the more derived lineages of the *Pachycondyla* genus group, including *Igaponera*.

The degree of fusion of the laterotergite of the petiole and the petiolar node (char. 30) is a character that varies in ponerines. As here considered, the plates are partially fused (state 0), revealed by a suture along the margins. This character state is shared among *Igaponera* and its closely related lineages, plus *Mayaponera*. The opposite condition, where the plates are fully fused (state 1), is present in *Simopelta* and *Thaumatomyrmex*. Outside of the genus group, this latter trait is also present in *Rasopone* Schmidt & Shattuck, 2014, a morphologically similar lineage whose phylogenetic affinities within the Ponerinae are still unclear.

Despite showing variations across many ponerine genera, the outline of the velum on the strigil's calcar [also called "basoventral lamella" in Esteves & Fisher (2021), or just "basal lamella" in Keller (2011)], can be classified in easily discernible patterns among the *Pachycondyla* group lineages where this trait is well-developed. In *Neoponera*, the velum is mostly round at its base, except for *N. concava*, *N. schultzi*, and *N. venusta*, where it is subtriangular; in *Pachycondyla*, it is horizontally straight; and in *Igaponera curiosa*, it is slightly rounded, but similar to most *Neoponera*. These variations were not scored as character statements in our matrix, but we think they are phylogenetically informative and should be considered in future studies.

Finally, we concur with Esteves & Fisher (2021) in the sense that *I. curiosa* "conforms with the characters shared by *Neoponera* and *Pachycondyla*" (p. 103). In the next line, though, they remark: "In addition, the species possesses a stridulitrum on the pretergite of abdominal segment IV" (p. 103), citing Mackay & Mackay (2010). We thoroughly examined this region and can confirm that it is absent, as in all *Pachycondyla* species. In *Neoponera*, on the other hand, this structure is always present, either faintly or strongly impressed.

Identifying *Igaponera*

The queen of this species will run to couplet 6 in the key to Neotropical ponerine genera by Schmidt & Shattuck (2014), where it fits into *Pachycondyla* more than *Neoponera* because it lacks a stridulitrum, the arolia are not prominent, and there is no malar carina. Nonetheless, a number of *Neoponera* species also lack a malar carina, and some species show non-prominent arolia. In the key to ponerine genera for Colombia by Fernández & Guerrero (2019), *Igaponera* runs to couplet 13 but does not fit either of the two alternatives as it has the node shape described for *Pachycondyla* and not for *Neoponera*. In addition, *Igaponera* lacks the stout, spine-like hypopygial setae typical of *Pachycondyla*, which are also present in most species of the *Neoponera crenata* species-group, as noted also in Esteves & Fisher (2021). In the latest key to Neotropical ponerine genera by Esteves & Fisher (2021), *Igaponera* runs to couplet 18 leading to *Pachycondyla* and *Mayaponera*, but not exactly fitting either lead because it has a slit-shaped propodeal spiracle but lacks hypopygial aristate and spine-like setae. Its costate sculpture will immediately differentiate it from those genera, however.

As mentioned before, within the *Pachycondyla* group, *Igaponera* bears closest overall resemblance to *Mayaponera*, *Neoponera*, and *Pachycondyla,* but outside that genus group it is also morphologically similar to *Pseudoponera* and *Rasopone*. However, the following frequently used diagnostic traits of these genera are not found in *Igaponera*:

Mayaponera: Species in this genus have relatively smaller eyes placed anteriorly on the head, elongate mandibles with about 12 teeth, a rounded to oval propodeal spiracle, a scale-shaped petiole and no prora. *Mayaponera constricta* has relatively larger eyes than the other species in the genus, but they are flattened and do not attain the relative size present in *Igaponera.*

Neoponera: all the species in this genus have a stridulitrum on the abdominal pretergite IV, usually prominent arolia on the pretarsal claws, and many species bear distinct malar carinae. This genus shows great morphological variation and indeed some of the diagnostic characters for *Igaponera* can also be found in *Neoponera*.

Pachycondyla: this genus has smaller eyes placed anteriorly on the head, elongate mandibles with 7-11 teeth, frequently an anterolateral carina on the pronotum, and no arolia on the pretarsal claws. *Pachycondyla* species generally have a cuboid petiolar node approximating the shape in *Igaponera*, but the node in this genus, in lateral view, has a straight anterior petiolar margin and a weakly convex to almost flat dorsal margin that is higher than the posterior margin, usually with the posterior face curving anteriorly near the apex; the length of the propodeal declivitous margin, in lateral view, is relatively longer than in *Igaponera*, and forms a more open obtuse angle with the dorsal margin.

Pseudoponera: these are much smaller ants with small eyes placed on the anterior part of the head, the mandible has 5–7 teeth, the propodeal spiracle is rounded, the petiolar node is scale-shaped, the pretarsal claws lack arolia, the dorsum of the propodeum narrows anteriorly, and the clypeus often bears a transverse carina.

Rasopone: ants in this genus have elongate mandibles with an average of 12 teeth, relatively small ocelli, round or ovoid propodeal spiracles, the petiolar sternite with a posterior transverse groove, and no prora; the petiolar node is usually scale-shaped, but if thickened, then the anterior and posterior faces are flattened and parallel to each other (Longino & Branstetter 2020).

Comparative morphology of diagnostic characters

Perhaps the most outstanding diagnostic morphological feature of this ant is the costate sculpturing that covers most of its body, particularly on the cephalic dorsum, most of the mesosoma, and the petiole. Such sculpture is more typical in Neotropical *Gnamptogenys* Roger, 1863, but not in Ponerinae. There are no other Neotropical ponerines that bear such sculpturing extensively over their bodies and the only species that come close are two *Neoponera* species: *N. lineaticeps* and *N. magnifica*. The former species has a patch of costulae on the median frons only, and the latter has costulae on the cephalic and pronotal dorsum, and sometimes variably developed on the mesonotum. The costulae of these species are relatively narrower and shallower than in *I. curiosa*. Ponerines from other biogeographic regions with similar costulae include the genus *Diacamma* Mayr, 1862, *Paltothyreus tarsatus*, an African species with costulae on the promesonotum only, and the Indomalayan *Odontoponera* Mayr, 1862 which bear costulae on the head and mesosomal dorsum.

The antennal scape in *Igaponera* fails to reach the posterior cephalic margin (by less than one apical width) when pulled back. In *Neoponera*, the scape usually surpasses the posterior cephalic margin by at least one apical width. Only two species in the *N. laevigata* species group and *N. fisheri* have a scape that fails to reach the posterior cephalic margin.

The mandibles in *Igaponera* are relatively short and robust, with short, robust teeth and denticles, and the apical tooth is not noticeably longer than the preceding teeth. This gives the mandibular apex a blunt shape, unlike in *Neoponera* and many other ponerines in which an acute apical angle gives the mandible an elongate triangular shape. Exceptions are found in *N. magnifica*, *N. fisheri*, and *N. luteola*, all with a mandible not as elongate as in other *Neoponera*, but they still have an acute apical angle, distinctly different from the state in *Igaponera. Pseudoponera* mandibles appear not as elongate as in the other genera, but they do not exhibit the condition in *Igaponera*. This morphology suggests *Igaponera* may use their mandibles for chewing upon hard items, perhaps heavily armored prey.

The base of the hypostomal tooth is recessed below the surrounding surface of the hypostomal bridge in *I. curiosa*, and the tip of the tooth is directed vertically to the surrounding cephalic surface. In the studied specimens of *Neoponera, Pachycondyla*, *Mayaponera*, *Rasopone*, and *Pseudoponera*, this base is approximately on the same plane as the surrounding ventral cephalic surface and the tooth itself is not raised vertically but projects anteriorly or anterolaterally. In most *Neoponera*, the hypostomal margin forms an arch when the head is seen anteriorly, with the median region higher than the lateral extremities. The lateral hypostomal tooth projects anterad as a continuation of this arch.

The metapleural gland opening in *Igaponera* is enclosed dorsally by a flange that conceals it in dorsal view. Such a structure is absent in the studied specimens of *Neoponera, Pachycondyla*, *Rasopone*, *Mayaponera* and *Pseudoponera*, and the gland opening in these taxa can be partially seen in dorsal view. The lack of a dorsal lobe or carina that hides the metapleural gland opening is considered a trait of Ponerinae by Bolton (2003). Nevertheless, a similar variation of this flange is found in *Simopelta pergandei* and *S. oculata* (ANTWEB1008588, SEM images), but the structure of the gland opening is completely different compared to all the aforementioned genera, suggesting independent development from that of *Igaponera*.

Mackay & Mackay (2010) described the existence of a stridulitrum for this species but we examined the fourth abdominal pretergite at 60× and were not able to detect a structure we could identify as such. We did find a small irregularly-shaped patch that changes shape depending upon the angle of incident light, but its structure and size do not suggest a stridulitrum as it lacks the typical iridescence. In a few *Neoponera*, for example *N. commutata* and *N. laevigata*, the stridulitrum may not form a typical triangular-shaped structure, but it is still recognizable as a stridulitrum. It is shaped as a relatively much narrower, sub-triangular, dashed patch with iridescence. The presence of a stridulitrum is a diagnostic character for *Neoponera* (Schmidt & Shattuck 2014), prompting Esteves & Fisher (2021) to use its supposed presence in *Igaponera* as support for transfering the species from *Pachycondyla* to *Neoponera*.

Neoponera, *Pachycondyla*, *Mayaponera*, *Pseudoponera*, and *Rasopone* have a variable number of setae of differing development on the apex of the meso- and metatibiae, but the setae are totally absent in *Igaponera*. Also, the apical margin of each meso- and metatarsomere in the aforementioned genera usually bears stout setae. These setae have a polished appearance and are typically darker than the surrounding pilosity, suggesting greater sclerotization and stiffness, regardless of their relative thickness. The apices of the meso- and metatarsal segments in *Igaponera* have elongate, lighter colored setae that are not polished but bear a sheen. Some are slightly arched, and overall their appearance suggests diminished stiffness. Similar setae can be found in species such as *Pseudoponera stigma* and *Neoponera crenata.* A dorsal transverse strip of rugosity adjacent to the third abdominal pretergite, just posterad to the helcium, is present in *Igaponera* and absent in *Pachycondyla*, *Mayaponera*, *Pseudoponera stigma*, and most *Neoponera*, though *Neoponera foetida*, *N. latinoda, and N. inversa* have rugulae in this region. *Mayaponera arhuaca* and *R. lunaris* exhibit a narrow band of very fine rugosity in this region.

Notes on the habitat of *I. curiosa*

This ant was collected by Dr. Joachim Adis (1981) during a study of the arthropod fauna inhabiting the Rio Tarumã Mirim Igapó, a seasonally flooded, black water forest 20 km upstream from Manaus, close to where the Rio Tarumã Mirim empties into the Rio Negro. The type locality coordinates are 03°02′S, 60°17′W (-3.03, -60.28) according to Adis (1981: fig. 1), but these coordinates indicate a point 25 km west of the Eduardo Gomes International Airport of Manaus, not coinciding with the location of the collection site depicted in figures 1 & 2 from Adis (1981). Using the graphic location of both figures, the coordinates should be approximately -3.02, -60.17, a site 14 km west of the airport, barely 20 m above sea level.

Adis sampled using pitfall traps, ground photo-eclectors and arboreal photo-eclectors. The arboreal traps were designed to catch insects moving on tree trunks. His specimens were killed and then preserved for an indeterminate amount of time in an aqueous solution of picric acid. Since the seasonal flooding permits only a scant layer of leaf litter to accumulate at the end of the dry season, it is assumed this species is more likely an arboreal rather than a leaf-litter or subterranean ant, despite having very small arolia.

Due to its proximity to Manaus, the area where this specimen was found is frequently used for research purposes by academic programs, such as those of INPA. The voucher specimens collected by Adis are deposited in the INPA collection. One of us searched for additional specimens there, but none could be found, suggesting it is a relatively rare species or has a biology that keeps it from being frequently collected by the usual field techniques. The large eyes could imply activity in low-light conditions, such as during the night, but also this is a functional trait linked to flight, for example, during mating and nest search (Julian & Gronenberg 2002; Peeters *et al.* 2013).

Conclusions

While there are several distinct characters that permit diagnosing this genus, it is much harder to recognize which of these might constitute apomorphies. The likely candidates seem to be the presence of a cuticular flange that conceals the metapleural gland opening in dorsal view, the vertically standing hypostomal tooth, the stout mandibular shape with a blunt apex, and perhaps the relatively long, erect tarsal setae. Given the morphological variability of *Neoponera*, the above characters, plus the lack of apical meso- and metatibial setae in *Igaponera*, are other characters useful in separating these two genera. Our results support placing *Igaponera* in a close relationship to both *Neoponera* and *Pachycondyla* in the tribe Ponerini. Further analyses, hopefully integrating molecular and biological data of *Igaponera*, will be required to get a more detailed picture about its evolution in the ponerine phylogeny. We expect that additional specimens of this genus may eventually be collected or found in collections, perhaps misidentified as *Gnamptogenys*. For now, this is all we have. We encourage our colleagues in Amazonas and Pará, particularly those in Manaus, to make the effort in procuring more of these ants. Males, workers, and larvae remain to be described and their whole biology awaits study.

Acknowledgments

We are grateful to: Brian Brown and Weiping Xie of the LACM for their help in making the specimen available for study; Giar-Ann Kung of the LACM for taking additional images; Rodolfo Probst (University of Utah) for trying to coax DNA out of the specimen; Ibsen Martinsen (Max-Planck-Institut für Evolutionsbiologie) for help with bibliography and information regarding Joachim Adis; Itanna Fernandes (INPA) for her help in searching the INPA voucher collection and the ant collection; Rodrigo Feitosa and an anonymous reviewer for their thoughtful comments on the manuscript. Funding for this research was provided by PRINT/UFPR – CAPES (Projeto 88887.311853/2018-00) to JEL, CNPq (Projeto 870531/1997-2, processo 140728/2020-1) to FM, and USA National Science Foundation grant DEB-1932405 (Ants of the World) to JL. AT is thankful to the Escuela Politécnica Nacional (Ecuador) and to CNPq (Projeto 140995/2020-0).

References

Adis J. 1981. Comparative ecological studies of the terrestrial arthropod fauna in Central Amazonian inundation forests. *Amazoniana* 7: 87–173.
Available from http://hdl.handle.net/21.11116/0000-0004-6A95-D [accessed 19 May 2022].

Akaike H. 1973. Information theory and an extension of the maximum likelihood principle. *In*: Petrov B.N. & Csaki F. (eds) *2nd International Symposium on Information Theory*: 267–281. Akademia Kiado, Budapest. Available from https://link.springer.com/chapter/10.1007/978-1-4612-1694-0_15 [accessed 19 May 2022].

Anisimova M., Gil M., Dufayard J.F., Dessimoz C. & Gascuel O. 2011. Survey of branch support methods demonstrates accuracy, power, and robustness of fast likelihood-based approximation schemes. *Systematic Biology* 60 (5): 685–699. https://doi.org/10.1093/sysbio/syr041

Bolton B. 2003. Synopsis and classification of Formicidae. *Memoirs of the American Entomological Institute* 71: 1–370. Available from https://www.antcat.org/references/130789 [accessed 19 May 2022].

Branstetter M.G. & Longino J.T. 2022. UCE phylogenomics of New World *Cryptopone* (Hymenoptera: Formicidae) elucidates genus boundaries, species boundaries, and the vicariant history of a temperate–tropical disjunction. *Insect Systematics and Diversity* 6 (1): 1–23.
https://doi.org/10.1093/isd/ixab031

Branstetter M. G., Longino J.T., Ward P.S. & Faircloth B.C. 2017. Enriching the ant tree of life: Enhanced UCE bait set for genome-scale phylogenetics of ants and other Hymenoptera. *Methods in Ecology and Evolution* 8 (6): 768–776. https://doi.org/10.1111/2041-210X.12742

Delsinne T., Serna F.J., Leponce M. & Boudinot B.E. 2019. Glosario de morfología. *In*: Fernández F., Guerrero R.J. & Delsinne T. (eds) *Hormigas de Colombia*: 387–457. Universidad Nacional de Colombia, Bogotá. Available from https://antcat.org/references/143440 [accessed 19 May 2022].

Esteves F.A. & Fisher B.L. 2021. *Corrieopone nouragues gen. nov.*, *sp. nov.*, a new Ponerinae from French Guiana (Hymenoptera, Formicidae). *ZooKeys* 1074: 83–173.
https://doi.org/10.3897/zookeys.1074.75551

Felsenstein J. 1985. Confidence limits on phylogenies: an approach using the bootstrap. *Evolution* 39 (4): 783–791. https://doi.org/10.1111/j.1558-5646.1985.tb00420.x

Fernández F. & Guerrero R.J. 2019. Subfamilia Ponerinae. *In*: Fernández F., Guerrero R.J. & Delsinne T. (eds) *Hormigas de Colombia*: 509–553. Universidad Nacional de Colombia, Bogotá.
Available from https://antcat.org/references/143446 [accessed 19 May 2022].

Goloboff P.A. 2014. Extended implied weighting. *Cladistics* 30: 260–272.
https://doi.org/10.1111/cla.12047

Goloboff P.A. & Catalano S.A. 2016. TNT version 1.5, including a full implementation of phylogenetic morphometrics. *Cladistics* 32: 221–238. https://doi.org/10.1111/cla.12160

Goloboff P. & Farris J. 2001. Methods for quick consensus estimation. *Cladistics* 17: S26–S34.
https://doi.org/10.1111/j.1096-0031.2001.tb00102.x

Goloboff P.A., Farris J.S., Källersjö M., Oxelman B., Ramírez M.J. & Szumik C.A. 2003. Improvements to resampling measures of group support. *Cladistics* 19: 324–332.
https://doi.org/10.1111/j.1096-0031.2003.tb00376.x

Harris R.A. 1979. A glossary of surface sculpturing. *Occasional Papers in Entomology* 28: 1–31.
https://doi.org/10.5281/zenodo.26215

Hoang D.T., Chernomor O., Von Haeseler A., Minh B.Q. & Vinh L.S. 2018. UFBoot2: improving the ultrafast bootstrap approximation. *Molecular Biology and Evolution* 35 (2): 518–522. https://doi.org/10.1093/molbev/msx281

Julian G.E. & Gronenberg W. 2002. Reduction of brain volume correlates with behavioral changes in queen ants. *Brain, Behavior and Evolution* 60 (3): 152–164. https://doi.org/10.1159/000065936

Kalyaanamoorthy S., Minh B.Q., Wong T.K., Von Haeseler A. & Jermiin L.S. 2017. ModelFinder: fast model selection for accurate phylogenetic estimates. *Nature Methods* 14 (6): 587–589. https://doi.org/10.1038/nmeth.4285

Keller R.A. 2011. A phylogenetic analysis of ant morphology (Hymenoptera: Formicidae) with special reference to the poneromorph subfamilies. *Bulletin of the American Museum of Natural History* 2011 (355): 1–90. https://doi.org/10.1206/355.1

Lattke J.E. 1994. Phylogenetic relationships and classification of ectatommine ants (Hymenoptera: Formicidae). *Entomologica Scandinavica* 25: 105–119.
Available from https://www.antcat.org/references/126814 [accessed 19 May 2022].

Longino J.T. & Branstetter M.G. 2020. Phylogenomic species delimitation, taxonomy, and 'bird guide' identification of the Neotropical ant genus *Rasopone* (Hymenoptera: Formicidae). *Insect Systematics and Diversity* 4 (2): 1: 1–33. https://doi.org/10.1093/isd/ixaa004

Maddison W.P. & Maddison D.R. 2019. MESQUITE: a modular system for evolutionary analysis. Version 3.61. Available from http://www.mesquiteproject.org [accessed 19 May 2022].

MacKay W.P. & MacKay E. 2010. *The Systematics and Biology of the New World Ants of the Genus Pachycondyla (Hymenoptera: Formicidae)*. Edwin Mellen Press, Lewiston, New York.
Available from https://www.antcat.org/references/131785[accessed 19 May 2022].

Mariano C., Pompolo S., Gomes J. & Delabie J.H. 2011. Contribution of cytogenetics to the debate on the paraphyly of *Pachycondyla* spp. (Hymenoptera, Formicidae, Ponerinae). *Psyche* 2012. https://doi.org/10.1155/2012/973897

Markl H. 1973. The evolution of stridulatory communication in ants. *In: Proceedings of the International Congress IUSSI*. London. https://doi.org/10.1007/s00040-016-0470-6

Nguyen L.T., Schmidt H.A., Von Haeseler A. & Minh B.Q. 2015. IQ-TREE: a fast and effective stochastic algorithm for estimating maximum-likelihood phylogenies. *Molecular Biology and Evolution* 32 (1): 268–274. https://doi.org/10.1093/molbev/msu300

Nixon K.C. 2002. WINCLADA, ver. 1.00.08. Published by the author, Ithaca, NY.

Peeters C., Lin C.C., Quinet Y., Segundo G.M. & Billen J. 2013. Evolution of a soldier caste specialized to lay unfertilized eggs in the ant genus *Crematogaster* (subgenus *Orthocrema*). *Arthropod Structure & Development* 42 (3): 257–264. https://doi.org/10.1016/j.asd.2013.02.003

Perrault G.H. 2004. Étude morphoanatomique et biométrique du métasoma antérieur des ouvrières. Contribution à la systématique et à la phylogénie des fourmis (Hymenoptera: Formicidae). *In:* Taylor & Francis Group (eds) *Annales de la Société entomologique de France*: 291–371. https://doi.org/10.1080/00379271.2004.10697428

Pyron R.A., Burbrink F.T. & Wiens J.J. 2013. A phylogeny and revised classification of Squamata, including 4161 species of lizards and snakes. *BMC Evolutionary Biology* 13: 1–54. https://doi.org/10.1186/1471-2148-13-93

Richter A., Keller R.A., Rosumek F.B., Economo E.P., Hita Garcia F. & Beutel R.G. 2019. The cephalic anatomy of workers of the ant species *Wasmannia affinis* (Formicidae, Hymenoptera, Insecta) and its evolutionary implications. *Arthropod Structure & Development* 49: 26–49. https://doi.org/10.1016/j.asd.2019.02.002

Schmidt C.A. 2013. Molecular phylogenetics of ponerine ants (Hymenoptera: Formicidae: Ponerinae). *Zootaxa* 3647 (2): 201–250. https://doi.org/10.11646/zootaxa.3647.2.1

Schmidt C.A. & Shattuck S.O. 2014. The higher classification of the ant subfamily Ponerinae (Hymenoptera: Formicidae), with a review of ponerine ecology and behavior. *Zootaxa* 3817 (1): 1–242. https://doi.org/10.11646/zootaxa.3817.1.1

Schwarz G. 1978. Estimating the dimension of a model. *The Annals of Statistics* 6 (2): 461–464. https://doi.org/10.1214/aos/1176344136

Sereno P.C. 2007. Logical basis for morphological characters in phylogenetics. *Cladistics* 23 (6): 565–587. https://doi.org/10.1111/j.1096-0031.2007.00161.x

Wiemers M., Chazot N., Wheat C.W., Schweiger O. & Wahlberg N. 2020. A complete time-calibrated multi-gene phylogeny of the European butterflies. *ZooKeys* 938: 97–124. https://doi.org/10.3897/zookeys.938.50878

Wild A.L. 2005. Taxonomic revision of the *Pachycondyla apicalis* species complex (Hymenoptera: Formicidae). *Zootaxa* 834 (1): 1–25. https://doi.org/10.11646/zootaxa.834.1.1

Manuscript received: 27 October 2021
Manuscript accepted: 4 March 2022
Published on: 13 June 2022
Topic editor: Tony Robillard
Section editor: Gavin Broad
Desk editor: Fariza Sissi

Supplementary files

Supp. file 1. Characters and their states examined in the set of Ponerinae species represented in the phylogeny. https://doi.org/10.5852/ejt.2022.823.1817.7011

Supp. file 2. Scored data set of morphological characters (in .xlsx format) used in this study for constructing the phylogeny. https://doi.org/10.5852/ejt.2022.823.1817.7013

Supp. file 3. List of examined specimens (in .xlsx format), including the outgroups. https://doi.org/10.5852/ejt.2022.823.1817.7015

Supp. file 4. Consensus maximum parsimony trees showing bootstrap (Fig. 1A) and symmetric resampling (Fig. 1B) node supports. https://doi.org/10.5852/ejt.2022.823.1817.7017

Supp. file 5. TNT script (setk.run), used to calculate the value of the concavity function k, which in the present study was helpful in finding more resolved and congruent tree topologies.
https://doi.org/10.5852/ejt.2022.823.1817.7019